PROCEEDINGS OF SCIENCE

Precision spectroscopy of charmonium-like (exotic) XYZ states at PANDA/FAIR

Sensitivity study for width and line-shape measurements of the X(3872)

K. Götzen[2], R. Kliemt[2], Frank Nerling[1,2]*†, K. Peters[1,2], for the PANDA Collaboration

[1]*Goethe Univ. Frankfurt,* [2]*GSI Helmholtzzentrum für Schwerionenforschung GmbH, Darmstadt*

E-mail: F.Nerling@gsi.de

The PANDA experiment represents the central part of the hadron physics programme at the new Facility for Antiproton and Ion Research (FAIR) under construction at GSI/Darmstadt (Germany). The multi-purpose PANDA detector in combination with an intense and high-quality antiproton beam allows for coverage of a broad range of different aspects of QCD, and it is best suited for charmonium spectroscopy. We present a comprehensive PANDA Monte Carlo simulation study for precision resonance energy scan measurements, using the example of the charmonium-like $X(3872)$ state discussed to be exotic. Apart from the proof of principle for natural decay width and line-shape measurements of very narrow resonances, the achievable sensitivities are quantified for the concrete example of the $X(3872)$. The discussed measurement is uniquely possible with a $\bar{p}p$ annihilation experiment such as PANDA at FAIR.

XIII Quark Confinement and the Hadron Spectrum - Confinement2018
31 July - 6 August 2018
Maynooth University, Ireland

*Speaker.
†Email: F.Nerling@gsi.de

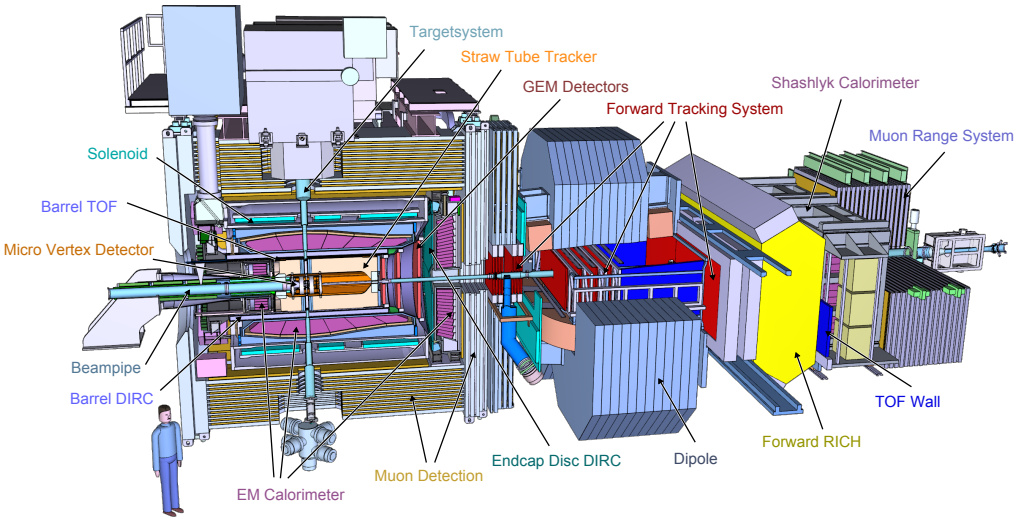

Figure 1: The proposed PANDA fixed-target experimental setup consists of a barrel spectrometer surrounding the target region and a forward spectrometer.

1. Introduction

The charmonium region offers unique possibilities to study bound states of the strong interaction, described by Quantum Chromodynamics (QCD), especially for searches for and studying exotic states. Based on potential models, charmonium states can successfully be described and predicted. Beneath the open-charm threshold, all the predicted states have been observed with the expected properties and excellent agreement is achieved between model calculations and experiment. Above the open-charm threshold, however, there are still many predicted states that have not yet been discovered, and, surprisingly, more than 20 unexpected states have been observed since 2003. Interesting examples of these so-called (exotic) charmonium-like "XYZ" states are the $X(3872)$ observed by Belle [1] in 2003, the $Y(4260)$ and $Y(4360)$, both discovered by BaBar using initial state radiation (ISR) [2, 3], and the charged state $Z_c(3900)^{\pm}$ discovered by BESIII [4], shortly after confirmed by Belle [5], that is a manifestly exotic state; for a recent overview see e.g. [6]. For the first of these unexpected states, the narrow $X(3872)$, only an experimental upper limit on the decay width of $\Gamma < 1.2\,\mathrm{MeV}/c^2$ exists [7], provided by the Belle experiment. For understanding the nature of this resonance, an absolute decay width measurement with sub-MeV resolution has to be performed, which can be done in a $\bar{p}p$ annihilation experiment.

2. The PANDA experiment at FAIR

The PANDA experiment dedicated to hadron physics [8], will be one of the main pillars at FAIR currently under construction in Darmstadt, Germany. The physics programme comprises hadron spectroscopy in the charm and light quark region, nucleon structure, hyper nuclear and strangeness production physics, and also studies of in-medium modifications of charm in nuclear matter will be part of the programme. The multi-purpose fixed-target PANDA experiment comprises a barrel detector surrounding the target region and a forward spectrometer (Fig. 1), ensuring

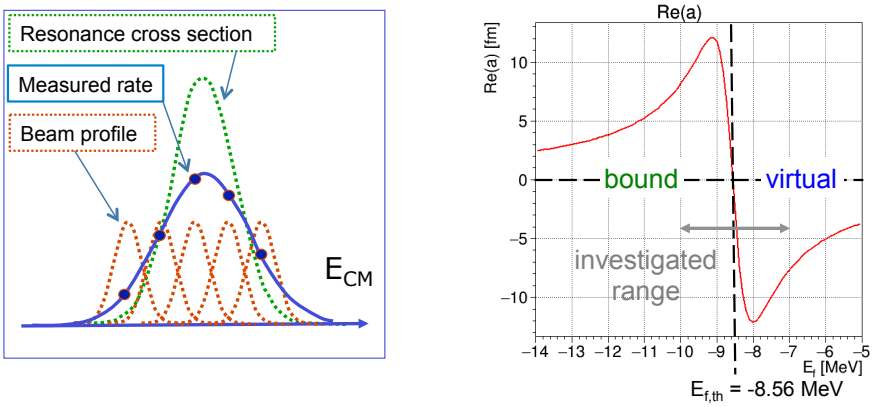

Figure 2: *Left:* Schematic of a resonance scan energy scan: The measured event rate (black data curve, blue line) is a convolution of the known beam profile and the underlying true energy dependent resonance cross-section (green dashed line). *Right:* Via the Flatté parameter E_f of the line-shape model the two scenarios of a bound molecular versus a virtual state can be distinguished.

an almost 4π acceptance with excellent tracking, vertexing, particle identification and calorimetry. Directly located at the High Energy Storage Ring (HESR), the PANDA experiment will be provided with an antiproton beam of momenta from 1.5 to 15 GeV/c for antiproton-proton annihilation reactions, translating to an directly accessible invariant mass range from about 2.2 up to 5.5 GeV/c^2. The HESR will offer two modes of operation. The High Resolution (HR) mode is optimised for beam momentum resolution, with a beam momentum spread of $\Delta p/p = 2\times10^{-5}$ and a luminosity of $\mathscr{L} = 2\times10^{31}$ cm^{-2}s^{-1}, whereas the High Luminosity mode, with a larger beam momentum spread $\Delta p/p = 1\times10^{-4}$, will have an optimised luminosity of 2×10^{32} cm^{-2}s^{-1}. In the initial phase (P1), the antiproton beam is expected to be available with $\Delta p/p = 5\times10^{-5}$ and $\mathscr{L} = 1\times10^{31}$ cm^{-2}s^{-1}.

3. Resonance energy scans of narrow resonances

One of the main advantages of using antiprotons is that in $\bar{p}p$ annihilation, PANDA has access to all fermion-antifermion J^{PC} quantum numbers in direct formation. This is not the case in e^+e^- annihilation, where the hadronic system directly produced in formation is restricted to those of the virtual photon ($J^{PC} = 1^{--}$) acting as a spin filter. The PANDA experiment will reach a very precise mass and width resolution by the technique of an energy resonance scan (Fig. 2, left) even for resonances with $J^{PC} \neq 1^{--}$, such as the $X(3872)$. At PANDA, we will have a cooled antiproton beam with excellent energy resolution, and thanks to the small and well controlled beam momentum spread $\Delta p/p$, we can scan the beam energy in the centre-of-mass energy (E_cms) range of interest, *i.e.* where a narrow resonance has been observed, and measure the energy dependent event yield. De-convolution of the known beam profile delivers an energy dependent resonance cross-section measurement at high precision.

We performed a comprehensive Monte Carlo (MC) sensitivity study for absolute decay width and line-shape measurements with PANDA, using the example of the narrow $X(3872)$ state with $J^{PC} = 1^{++}$ [9] that is discussed to be a molecular $\bar{D}^{*0}D^0$ bound system, see *e.g.* [10]. Apart from a simple Breit-Wigner decay width Γ measurement, we have studied in addition the feasibility to

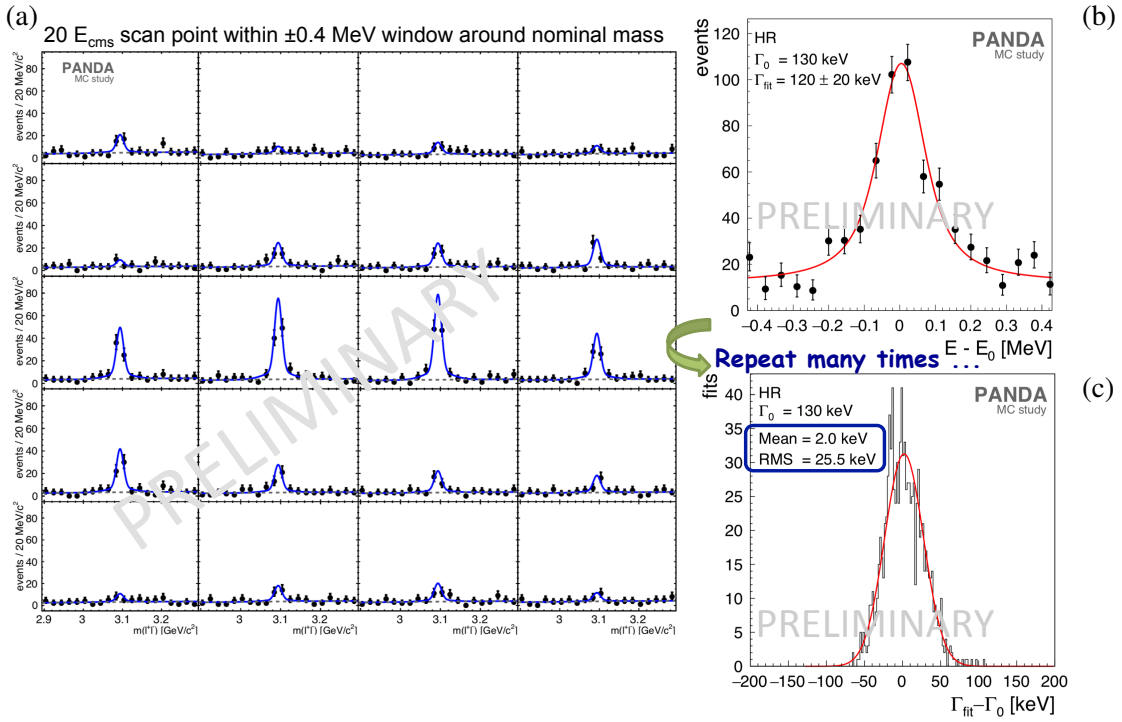

Figure 3: Illustration of a simulated toy MC experiment example ($\sigma_S = 100$ nb, Breit-Wigner width $\Gamma_0 = 130$ keV, two days of data taking per E_{cms} position, HR mode). *(a)* Simulated and reconstructed invariant di-lepton spectra at each energy scan positions (going from left to right, top to bottom step-wise through the energy range $(E - E_0)$. *(b)* The resultant energy dependent event yield distribution fitted with a function to extract the parameter of interest, here the Breit-Wigner width Γ, around the nominal centre-of-mass energy $E_0 = 3.872$ GeV. *(c)* From the distribution of the extracted parameter Γ_{fit} compared to the input value Γ_0 for 1000 toy MC experiments, the expected precision (root-mean-square RMS of the distribution) and the accuracy (shift Mean of the distribution) is estimated.

measure the line-shape as proposed in [11, 12] to distiniguish a molecular bound state from a virtual state scenario. According to this model, the corresponding line-shapes are defined involving the $\bar{D}^{*0}D^0$ scattering length, whereas the Flatté energy E_f determines the state to be a bound or a virtual state. The real part of the complexe scattering length is shown for illustration in Fig. 2, right, and the investigated range around the treshold value $E_{f,th} = -8.56$ MeV is indicated.

Based on realistic numbers of signal reconstruction efficiencies as obtained from a Geant-based PANDA MC simulation for the reaction $\bar{p}p \to X(3872) \to J/\psi\pi^+\pi^-$, with the J/ψ decaying to two leptons l^+l^-, namely $\mu^+\mu^-$ and e^+e^- (of 15.2 % and 12.2 %, respectively), and for non-resonant background without the $X(3872)$ being produced (3.0 % and 2.8 %), and corresponding (generic) background suppressions (of $4.5 \cdot 10^{-10}$ and $1.0 \cdot 10^{-10}$), experimentally measured branching ratios [13] and background cross-sections [14, 15] involved, we studied the achiveable performances at PANDA for 40 E_{cms} scan points and 80 days of beam time. The parameters varied in each toy MC experiment are the input assumptions on the signal production cross-section σ_S and either the decay width Γ_0 or the $E_{f,0}$ parameter. Each combination of (Γ_0, σ_S) or $(E_{f,0}, \sigma_S)$ has been simulated for the three different HESR operation mode (P1, HR, HL) conditions of energy resolution and luminosity.

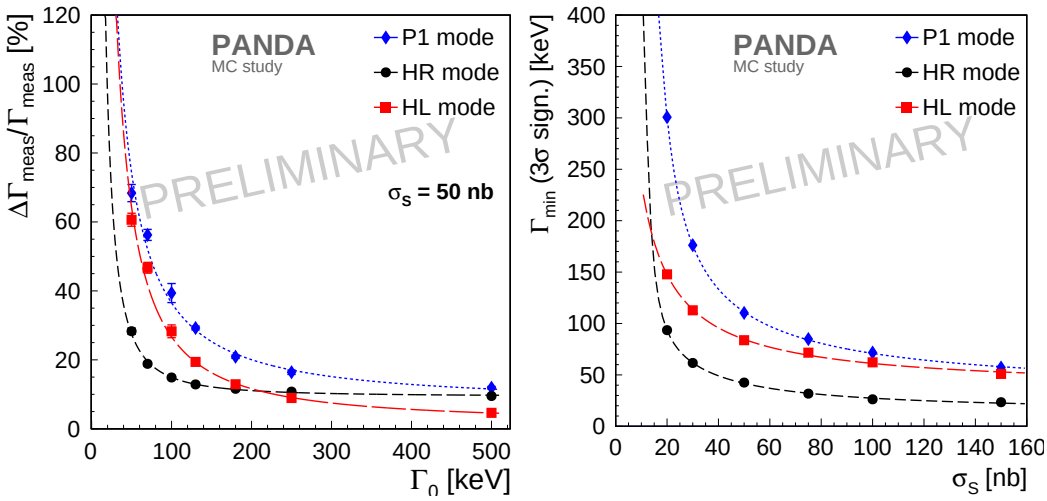

Figure 4: *Left:* Sensitivity for an absolute (Breit-Wigner) decay width measurement in terms of relative accuracy, at which an assumed input decay width Γ_0 can be measured for an assumed input signal production cross-section $\sigma_S = 50\,\text{nb}$. *Right:* Minimum decay width Γ_{min} that can be measured with an relative accuracy of 33 % as a function of the assumed input σ_S.

For illustration, the simulated di-lepton invariant mass spectra are exemplarily shown for a simulated energy scan experiment at 20 different E_{cms} scan points within a 0.8 MeV mass window around the nominal mass of the $X(3872)$ (Fig. 3). The spectra are sorted for an increasing E_{cms} (Fig. 3, a). Each stamp plot is fitted by a maximum-likelihood fit and the resultant energy dependent event yield measurement for this example of 20 scan points is plotted (Fig. 3, b). The given line-shape model, in this example the Breit-Wigner width Γ, is fitted and the parameter of interest (Γ) is determined. Repeating such toy MC experiment and measurement many times, we get an estimate of the uncertainties (Fig. 3, c).

In the following, the results of achievable sensitivities obtained from such toy MC experiments for natural decay width and line-shape measurements based on 40 energy scan points and two days of data taking at each position are summarised and discussed.

4. Performances for absolute decay width and line-shape measurements

The results obtained from the sensitivity study for a natural decay width measurement are summarised in Fig. 4. The achievable sensitivity is defined based on the obtained RMS and mean (Fig.3, c) as the relative accuracy

$$\frac{\Delta\Gamma_{\text{meas}}}{\Gamma_{\text{meas}}} := \frac{\text{RMS}}{\text{Mean} + \Gamma_0} \,,$$

at which an input decay width Γ_0 can be measured. It is exemplarily shown for the assumed signal production cross-section $\sigma_S = 50\,\text{nb}$ in Fig. 4 (left). The larger the input decay width Γ_0, and also the signal cross-section σ_S, the more precise is the achievable measurement, as expected. The achievable, interpolated relative uncertainity is better than about 10 % for Γ_0 larger than about 200 keV for the anticipated HL operation mode of the accelerator. For input decay widths smaller

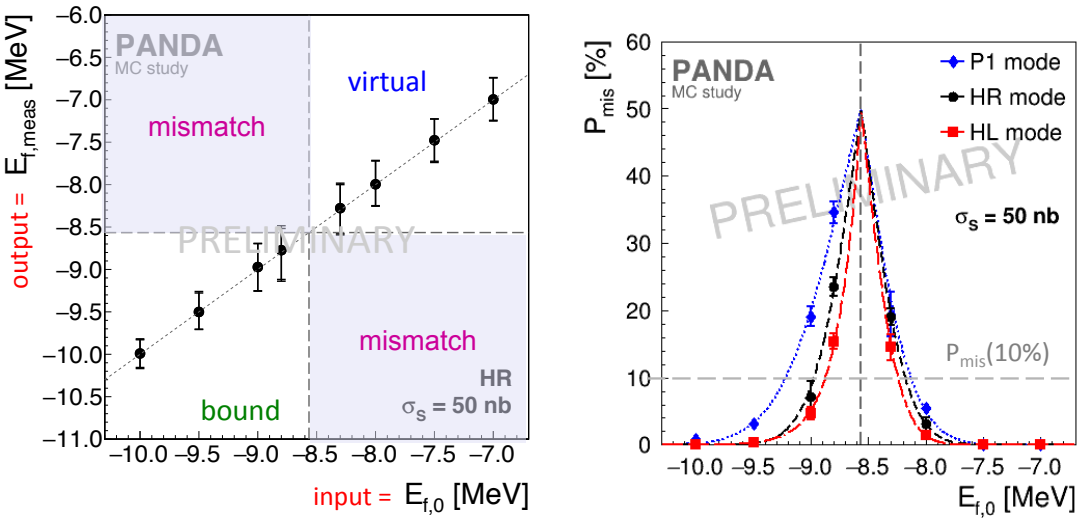

Figure 5: Sensitivity for the line-shape measurements via the E_f parameter (Molecule case) to distinguish between a bound and a virtual state scenario, exemplarily shown for an assumed input signal production cross-section $\sigma_\mathrm{S} = 50\,\mathrm{nb}$, HR mode. *Left:* Measured E_f versus the input parameter $E_{\mathrm{f},0}$ with the treshold value $E_{\mathrm{f,th}} = 8.56\,\mathrm{MeV}$ defining the two scenarios indicated as dashed (horiziontal and vertical) lines. *Right:* Sensitivity in terms of mis-identification probability P_mis versus the input Flatté parameter $E_{\mathrm{f},0}$.

than about 200 keV, the HR mode allows for more accurate measurements, whereas the HL mode is superior for input decay widths larger than about 200 keV.

A more compressed presentation of the results extracted from the $\Delta\Gamma_\mathrm{meas}/\Gamma_\mathrm{meas}$ versus Γ_0 plots from all six different signal cross-section assumptions $\sigma_\mathrm{S} = 20, 30, 50, 75, 100, 150\,\mathrm{nb}$ is given by the sensitivity plot for a 33 % relative error (3σ) measurement of the Breit-Wigner width (Fig. 4, right). For example extracted from Fig. 4 (left) for $\sigma_\mathrm{S} = 50\,\mathrm{nb}$, the minimum decay widths Γ_min that can be measured at 3σ accuracy is about $\Gamma_0 = 40\,\mathrm{keV}$ (HR), $\Gamma_0 = 80\,\mathrm{keV}$ (HL) and $\Gamma_0 = 110\,\mathrm{keV}$ (P1), respectively. Whereas a sub-MeV resolution is already feasible with P1, we find the HR mode superior over the investigated σ_S range.

For the case of line-shape measurements and distinction between a bound versus a virtual state scenario via the E_f parameter, a compilation of the measured $E_\mathrm{f,meas}$ as a function of the input parameter $E_{\mathrm{f},0}$ is exemplarily given in Fig. 5 (left). Here, the sensitivity is defined as the mis-identification probability

$$P_\mathrm{mis} := N_\mathrm{mis}/N_\mathrm{MC} \quad ,$$

where N_mis is the fraction of the number N_MC of MC simulated scan experiments performed (for a given parameter setting), for which the resulting fitted parameter $E_\mathrm{f,meas}$ is found on the opposite site of the threshold energy $E_\mathrm{f,th}$ than the corresponding input $E_{\mathrm{f},0}$. Those results are located in the areas indicated as "mismatch" region in Fig. 5 (left), and lead to mis-identification of the true nature, namely confusing the bound state with the virtual state scenario and vice versa. The resulting P_mis as a function of the input parameter $E_{\mathrm{f},0}$ is shown for the input signal production cross-section of $\sigma_\mathrm{S} = 50\,\mathrm{nb}$ for the theee different HESR operation modes in Fig. 5 (right). The larger the difference

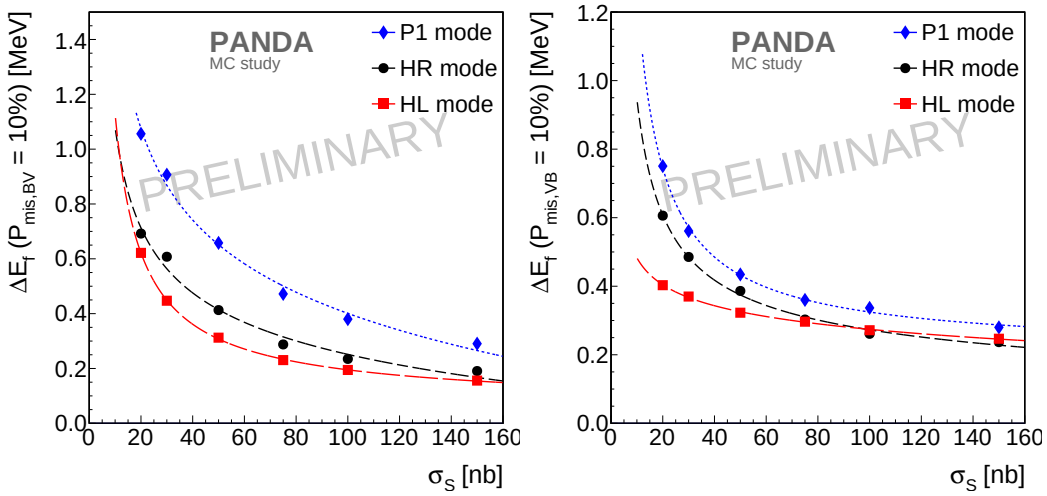

Figure 6: Sensitivity for line-shape measurements via the E_f parameter (Molecule case) to distinguish between a bound and a virtual state scenario (*left*) in terms of mis-identification to mis-identify a bound as a virtual state (*left*) and vice versa *(right)*.

$\Delta E_\mathrm{f} := |E_{\mathrm{f},0} - E_{\mathrm{f,th}}|$ and also the higher the input cross-section of σ_S, the lower is the resultant P_mis, and thus, the better the achievable performance.

The P_mis sensitivity results for the molecule case are also more compressed presented in Fig. 6. This is done in terms of ΔE_f as a function of σ_S as extracted from the P_mis *vs.* $E_{\mathrm{f},0}$ plots at $P_\mathrm{mis} = 10\,\%$ for all six different signal cross-section assumptions, exemplarily shown for $\sigma_\mathrm{S} = 50\,\mathrm{nb}$ (Fig. 5, right). They are separately shown for the case of a bound state being wrongly identified to be a virtual state at $P_\mathrm{mis,BV} = 10\,\%$, and for a virtual state being wrongly identified to be a bound state at $P_\mathrm{mis,VB} = 10\,\%$, respectively (Fig. 6).

5. Summary and conclusions

We performed a comprehensive MC sensitivity study for resonance energy scans of narrow states with the PANDA experiment. Experiments for measurements of natural decay widths and of line-shapes have realistically been simulated and analysed. The achievable performances have been quantified for the example of the famous $X(3872)$ state discussed to be of exotic nature.

For both, the natural decay width and the molecular line-shape scenario, the sensitivities have been studied for three anticipated HESR accelerator operation modes (P1, HL, HR), each based on an assumed data-taking time of 80 days equally distributed over 40 energy scan points.

The feasibility for sub-MeV resolution in absolute decay width measurements has been shown for a large parameter space of assumed signal production cross-sections. Moreover, a proof of principle for an experimental distinction between a bound state and a virtual state scenario for the $X(3872)$ has been provided based on measurements of line-shapes characterised by the dynamical Flatté energy paramter E_f.

References

[1] S.K. Choi *et al.* (Belle Collaboration), Phys. Rev. Lett. 91, 262001 (2003).

[2] B. Aubert *et al.* (BaBar Collaboration), Phys. Rev. Lett. 95, 142001 (2005).

[3] B. Aubert *et al.* (BaBar Collaboration), Phys. Rev. Lett. 98, 212001 (2007).

[4] M. Ablikin *et al.* (BESIII Collaboration), Phys. Rev. Lett. 110, 252001 (2013).

[5] Z.Q. Liu *et al.* (Belle Collaboration), Phys. Rev. Lett. 110, 252002 (2013).

[6] R.F. Lebedev, R.E. Mitchell and E.S. Swanson, arXiv:1610.04528v2 [hep-ex].

[7] S.-K. Choi *et al.* (Belle Collaboration), Phys. Rev. D 84, 052004 (2011).

[8] The PANDA Collaboration, arXiv:0903.3905 [hep-ex]

[9] R. Aaij *et al.* (LHCb Collaboration), Phys. Rev. Lett. 110, 222001 (2013).

[10] F. K. Guo *et al.*, Rev. Mod. Phys. 90, 015004 (2018).

[11] C. Hanhart *et al.*, Phys. Rev. D 76, 034007 (2007).

[12] Yu. S. Kalashnikova *et al.*, Phys. Atom. Nucl. 73, 1592-1611 (2010).

[13] K.A. Olive *et al.* (Particle Data Group), Chin. Phys. C 38, 090001 (2014), and 2015 update.

[14] Flaminio *et al.*, *Compilation of cross-sections*, CERN-HERA-84-01 (1984).

[15] G.Y.Chen *et al.*, Phys. Rev. D 77, 097501 (2008).